Numerical Simulation of Heat Transfer within a Cross Section of a Cylindrical Heat Pipe

Hichem Boulechfar[1,*], Selma Benzitouni[1]

[1] Faculty of Sciences, Department of Physics, University of M'sila, Med BOUDIAF-BP 166 M'sila 28000, Algeria

ARTICLE INFO	ABSTRACT
	The presented work concerned a computation of two-dimensional heat transfer by laminar natural convection in a heat pipe cross section. The cylindrical annular space was categorized into two cases, in the first case the space was filled with a Newtonian fluid and the second case filled with a fluid-saturated porous medium. The mathematical model was described by continuity, momentum and energy equations in the cylindrical coordinates system using Boussinesq's approximation and Brinkman's equation. The numerical simulation was carried out using Comsol Multiphysics software. The effects of Rayleigh number, aspect ratio and permeability on the temperature and the velocity fields were examined and results obtained were validated and found to be qualitatively in a good agreement with those in the literature.

1. Introduction

One of the most important research topics in our days, which posed a big challenging problem to a many engineers and researchers for decades ago, is the problem of efficient heat transfer. The heat pipe is one of the most remarkable achievements in heat management solutions that successfully implemented recently in varied industrial thermal management applications like electronic cooling, space craft thermal control, solar systems, automotive industry furnace applications [1]. It plays a very important role in the energy saving and show that it could manage a wide range of industrial applications with the indisputable advantage of being cheaper and more flexible in different sizes, shapes and designs. Currently, Considerable analytical and numerical studies have been made on heat pipes based on a variety of assumptions and problems to study their thermal performance which is greatly influenced by several factors such as geometry, dimensions, working fluids, filament materials, etc.

Jung and Joon [2] studied the steady-state analytical modeling of a loop heat pipe (LHP) equipped with a flat evaporator that was presented to predict the temperatures and pressures at each important part of the LHP evaporator. Albeshri *et al.,* [3] presented a numerical investigation

---

* Corresponding author.
E-mail address: hichem.boulechfar@univ-msila.dz

of the hydrodynamic behaviour of the laminar mixed convective flow of a hybrid nanofluid in the entrance region of a horizontal annulus. The SIMPLER numerical algorithm is adopted in the present study. Sun and Tien [4] studied thermal performance and characteristics of heat pipe. Ja *et al.,* [5] presented a numerical simulation of double diffusive natural convection flows within a cylindrical horizontal annular filled with a saturated porous medium. The study concerns the effect of different parameters governing the problem, namely, the Rayleigh number Ra, the Lewis number Le and the buoyancy ratio N, on both heat and mass transfer with the analysis of the flow structure changes for a radius ratio R=2. Abdulhafid *et al.,* [6] performed a numerical computational fluid dynamics (CFD) simulation for forced convection heat transfer of Al_2O_3 nanofluids in a circular pipe with constant heat flow is carried out. The convective heat-transfer coefficient, Nusselt number, and friction factor of a nanofluid are studied as a function of Reynolds number and particle volume fraction. Kumar *et al.,* [7] reported a theoretical and experimental study of a wire screen heat pipe computed thermal resistances at the external surface of the evaporator and condenser as well as inside the heat pipe, the theoretical study deals with the development of an analytical model based on thermal resistance network approach. Blet *et al.,* [8] presented a summary of heat pipe was described for the function of temperature homogenization then performed and identified their specificities, compared to other applications of heat pipes. Braga and Marcelo [9] presented a natural convection in concentric cylinders with a porous sleeve, analytical solutions obtained through perturbation method and Fourier transform solution. Boulechfar *et al.,* [10] studied numerically two-dimensional natural convection in an annular elliptical space fluid-saturated porous, by solving numerically the mass balance equations, momentum and energy, using Darcy's law, Boussinesq approximation, vorticity-stream function formulation and the finite volumes method for the discretization of partial derivative equations. Famouri [11] introduced a robust numerical scheme employed and developed to investigate transient and steady-state operation of cylindrical heat pipes with hybrid wick structure for high heat fluxes based on an incompressible flow model. Hussain and Isam [12] studied a numerical simulation method to analyze the performance of the heat pipe depended on four parameters namely, porosity, condenser evaporator lengths and radius of the heat pipe and the heat input, in terms of the absolute thermal resistance. Ma'a *et al.,* [13] studied and carried out experimentation on a heater in a concentric pipe with a straight construction is the general form. A heater is used to transfer the heat, and there is a cold fluid flow through the annulus. Simultaneously, cold fluid flows in the annulus using a closed system with six flow variations ranging from 2.5 GPM to 5 GPM. With the presence of cooling system used to maintain cold fluids at a constant temperature.

2. Model description

The physical domain is presented as an annulus space filled with porous medium known as wick structure. The transfer of thermal energy in the solid matrix and the fluid phase takes place by means of two different processes. Firstly, by means of conduction process that involves the transfer of thermal energy through the solid matrix of the porous medium. Secondly, by means of free convection involving the transfer of thermal energy in the annular space that contains a porous medium saturated with the working fluid (air). Figure 1 represents a cross section of a cylindrical heat pipe with reference to the radius of the outer and the inner cylinders R_i, R_o.
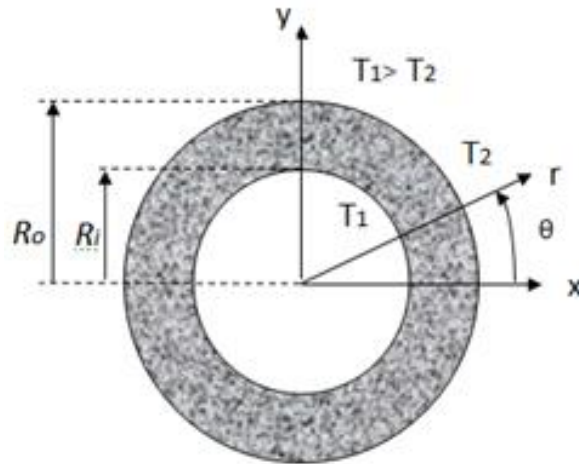
Fig. 1. Heat pipe cross section

The flow is assumed to be bidimensional, steady and laminar. The working fluid is presumed to be Newtonian and incompressible. The porous medium is considered homogeneous and isotropic. The Boussinesq approximation is applicable and the fluid physical properties are assumed constant except for the density.

Continuity equation

$$\frac{\partial U_r}{\partial r} + \frac{U_r}{r} + \frac{1}{r}\frac{\partial U_\theta}{\partial \theta} = 0 \tag{1}$$

Momentum equation

$$\rho\left(U_r\frac{\partial U_r}{\partial r} + \frac{U_\theta}{r}\frac{\partial U_r}{\partial \theta} - \frac{U_\theta^2}{r}\right) = -\frac{\partial P}{\partial r} + \mu\left(\frac{\partial^2 U_r}{\partial r^2} + \frac{1}{r}\frac{\partial U_r}{\partial r} + \frac{1}{r^2}\frac{\partial^2 U_r}{\partial \theta^2} - \frac{U_r}{r^2} - \frac{2}{r^2}\frac{\partial U_\theta}{\partial \theta}\right) + g\rho\cos\theta\,\beta(T - T_0) \tag{2}$$

$$\rho\left(U_r\frac{\partial U_\theta}{\partial r} + \frac{U_\theta}{r}\frac{\partial U_\theta}{\partial \theta} - \frac{U_r U_\theta}{r}\right) = -\frac{1}{r}\frac{\partial P}{\partial r} + \mu\left(\frac{\partial^2 U_\theta}{\partial r^2} + \frac{1}{r}\frac{\partial U_\theta}{\partial r} + \frac{1}{r^2}\frac{\partial^2 U_\theta}{\partial \theta^2} - \frac{U_\theta}{r^2} + \frac{2}{r^2}\frac{\partial U_r}{\partial \theta}\right) + g\rho\sin\theta\,\beta(T - T_0) \tag{3}$$

Energy equation

$$\rho\left(U_r\frac{\partial T}{\partial r} + \frac{U_\theta}{r}\frac{\partial T}{\partial \theta}\right) = \frac{\lambda}{C_p}\left(\frac{\partial^2 T}{\partial r^2} + \frac{1}{r}\frac{\partial T}{\partial r} + \frac{1}{r^2}\frac{\partial^2 T}{\partial \theta^2}\right) \tag{4}$$

The boundary conditions are expressed as following

The internal wall: r =R_i

$$U_r = U_\theta = 0, \qquad T = T_1 = T_{HOT}$$

The external wall: r =R_o

$$U_r = U_\theta = 0, \qquad T = T_2 = T_{COLD}$$

In order to control, measure and to reveal the controlling parameters it's recommended to obtain the dimensionless form of the modeling equations define based on the following characteristic quantities

$$A = \frac{R_0}{R_i}, \quad U_r^* = \frac{U_r}{\alpha/R_i}, \quad U_\theta^* = \frac{U_\theta}{\alpha/R_i}, \quad r^* = \frac{r}{R_i}, \quad P^* = \frac{P}{\rho(\frac{\alpha}{R_i})^2}, \quad T^* = \frac{(T-T_2)}{(T_1-T_2)}$$

Continuity equation

$$\frac{\partial U_r^*}{\partial r^*} + \frac{U_r^*}{r^*} + \frac{1}{r^*}\frac{\partial U_\theta^*}{\partial \theta} = 0 \tag{5}$$

Momentum equation

$$\left(U_r^* \frac{\partial U_r^*}{\partial r^*} + \frac{U_\theta^*}{r^*}\frac{\partial U_r^*}{\partial \theta} - \frac{U_\theta^{*2}}{r^*}\right) = -\frac{\partial P^*}{\partial r^*} + Pr\left(\frac{\partial^2 U_r^*}{\partial r^{*2}} + \frac{1}{r}\frac{\partial U_r^*}{\partial r^*} + \frac{1}{r^{*2}}\frac{\partial^2 U_r^*}{\partial \theta^2} - \frac{U_r^*}{r^2} - \frac{2}{r^{*2}}\frac{\partial U_\theta^*}{\partial \theta}\right) + Pr.Ra.\cos\theta\, T^* \tag{6}$$

$$\left(U_r^* \frac{\partial U_\theta^*}{\partial r^*} + \frac{U_\theta^*}{r^*}\frac{\partial U_\theta^*}{\partial \theta} - \frac{U_r^* U_\theta^*}{r}\right) = -\frac{1}{r^*}\frac{\partial P^*}{\partial \theta^*} + Pr\left(\frac{\partial^2 U_\theta^*}{\partial r^{*2}} + \frac{1}{r}\frac{\partial U_\theta^*}{\partial r^*} + \frac{1}{r^{*2}}\frac{\partial^2 U_\theta^*}{\partial \theta^2} - \frac{U_\theta^*}{r^{*2}} + \frac{2}{r^{*2}}\frac{U_r^*}{\partial \theta}\right) + Pr.Ra.\sin\theta\, T^* \tag{7}$$

Energy equation

$$\left(U_r^* \frac{\partial T^*}{\partial r^*} + \frac{U_\theta^*}{r^*}\frac{\partial T^*}{\partial \theta}\right) = \left(\frac{\partial^2 T^*}{\partial r^{*2}} + \frac{1}{r^*}\frac{\partial T^*}{\partial r^*} + \frac{1}{r^{*2}}\frac{\partial^2 T^*}{\partial \theta^2}\right) \tag{8}$$

The Brinkman constitutive model

$$-\frac{\mu}{K}\vec{U} = \left(\rho\vec{g} - \vec{\nabla}P\right) + \mu\nabla^2 U \tag{9}$$

3. Results

We represented our results in two main parts. The first part concerns the case where the physical space is filled with a Newtonian fluid and we illustrate results of the dimensionless temperature distribution and velocity field for a different Rayleigh number and aspect ratio values to examine their effects on the convective heat transfer and the flow motion within the annular cylindrical space. The fluid used is the air with Prandtl number $Pr=0.71$ and the Rayleigh number ranges from 10^3 to 10^7 for three values of the aspect ratio $A=1.2$, 2 and 3.

The second part concerns the case where the physical space is filled with fluid-saturated porous medium. Here we focused more on the permeability factor to examine its effect on the convective heat transfer and the flow motion, the porous medium permeability ranges from 10^{-1} to 10^{-5} m^2 with fixed Rayleigh number $Ra= 10^5$ and aspect ratio $A=2$.

3. 1 Validation

As a first objective we validated our results by comparing them with three analyses published in the literature. Our simulation parameters were taken equal to those in these works and the results were found to be relatively in a good agreement as shown in Figure 2-4.

Figure 2 shows the contours of the temperature and velocity field of published by Tahseen *et al.,* [14] for $Ra= 7.12\times10^2$. Both results are qualitatively similar in the whole annular space for the

temperature distribution which represents a conductive heat transfer and for the flow structure both results are showing the presence of two counter rotating cells.

Figure 3 shows a second comparison with numerical results of Yang and Song-Charng [15] for Ra=10^4 and Pr=1. Both results reproduced the same flow structure in the annular space in on hand, in the other hand the heat was not transferred with the same intensity of the convective mechanism especially in the upper side of the annular space. Figure 3 presents a third comparison using the reference Yuan *et al.,* [16]. The same temperature distribution was noticed with a slight difference in flow structure.

(a)   (b)
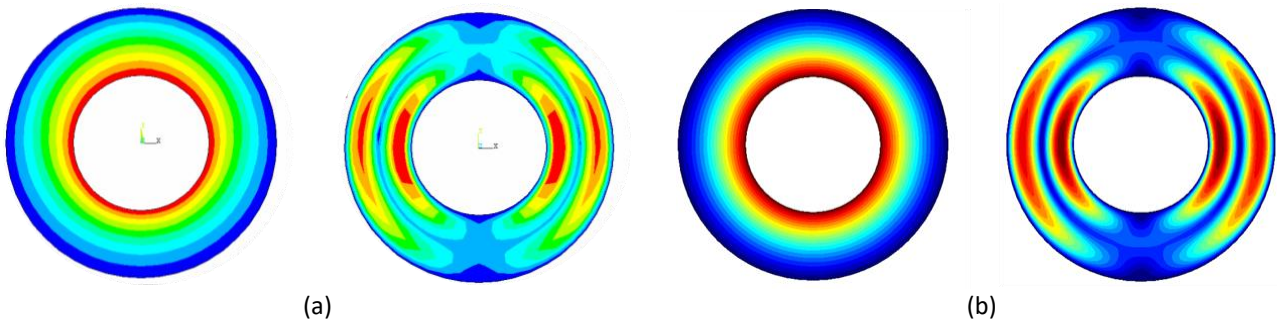
Fig. 2. Qualitative comparison of Isotherms and streamlines for Ra= $7.12x10^2$, Pr=0.71 and A=2, (a) [14] and (b) the present work

(a)   (b)
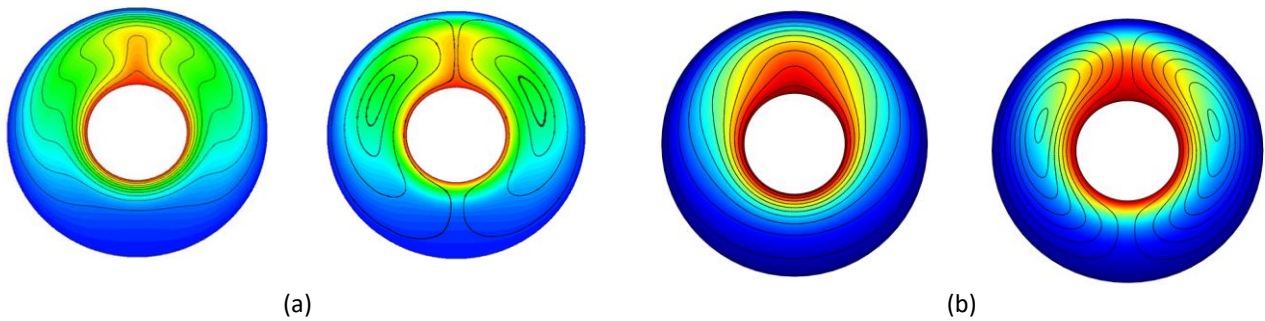
Fig. 3. Qualitative comparison of Isotherms and streamlines for Ra=10^4, Pr=1 and A=2.6, (a) [15] and (b) the present work

(a)   (b)
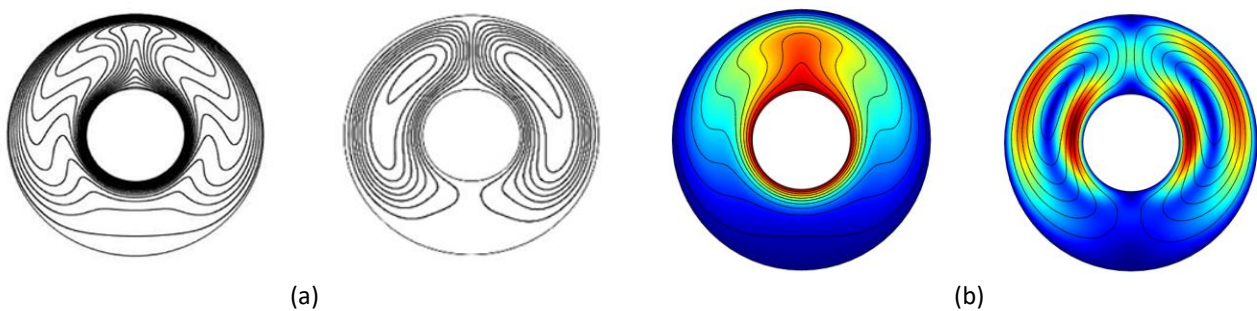
Fig. 4. Qualitative comparison of Isotherms and streamlines for Ra=5.10^4, Pr=0.71 and A=2.6, (a) [16] and (b) the present work

3. 2 Space Filled with a Fluid
3.2.1 Effect of Rayleigh number

Figure 5 represents the temperature distribution (isotherms) and velocity field (streamlines) with vectors for different values of Rayleigh number where the aspect ratio was kept constant (A=2). We can observe that these contours are symmetrical about the median fictitious vertical

plane in the annular space. The isotherms in Figure 5(a) for Ra=10^3 are concentric closed curves which coincide with the walls profile; in this case the temperature distribution is simply decreasing from the hot wall to the cold wall. The velocity field in the same figure shows that the flow is organized in two main cells that rotate very slowly in opposite directions. This is due to the upward movement of the fluid particles which heat up along the hot wall under the buoyancy effect related to temperature gradients and the downward movements of the fluid particles which cool along the cold wall under the gravity. The fluid motion is very slow and the dimensionless velocity values are relatively low. This mode of heat transfer is dominated by a pseudo-conductive regime for the case of low Ra values. With a further increase in Rayleigh number as shown in Figure 5(b) isotherms become distorted which means that the convective mode is taking place in the upper side of the annular space and the fluid motion is dominated by a buoyancy-driven flow. In the lower space, isotherms become very close to each other near the hot wall forming a boundary layer where the pseudo conduction still acting with a slight contribution of the convection far from this boundary layer.When the increase of Rayleigh number reaches Ra = 106 to Ra = 107 as shown respectively in Figure 5(c) and Figure 5(b) where a net intensification of the convective mode in the whole annular space was noticeable. Isotherms are completely changed from a circular concentric contours form to a wing form under the intensification of the flow motion structure which is formed by two counter rotating cells in the left and the right sides of the space.


(a) Ra=10^3 (b) Ra=10^5

(c) Ra=10^6 (d) Ra=10^7
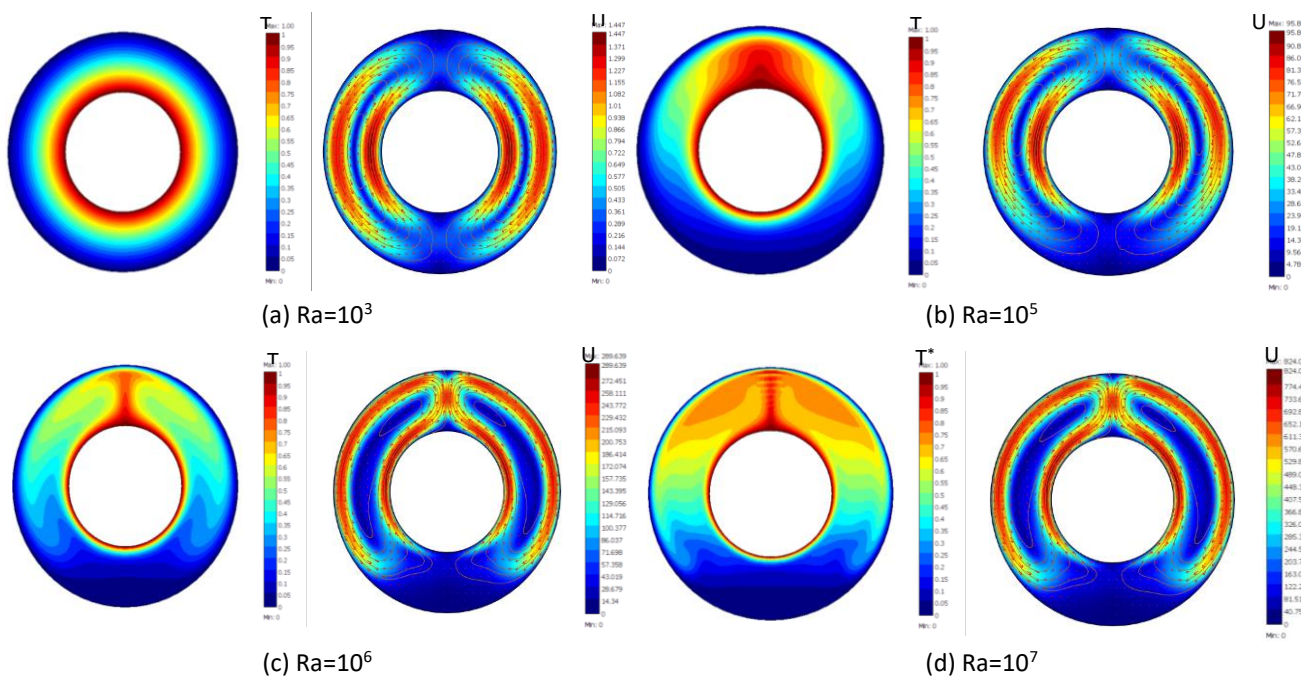
Fig. 5. Isotherms and streamlines for different values of Ra with aspect ratio A=2

3.2.2 Effect of aspect ratio

Figure 6 represents isotherms and streamlines for the same Rayleigh number Ra=10^5 and different Aspect ratios A=1.2, A=2, A=3. Figures illustrate that contours are symmetrical about the median fictitious vertical plane in the annular space and that the flow remains organized in two main cells that rotate in opposite directions. The isotherms in Figure 6(a) for A=1.2 are concentric closed curves which coincide perfectly with the walls profile; in this case the temperature distribution is simply decreasing from the hot wall to the cold wall. The velocity field in the same figure shows that the flow is organized in two main cells that rotate very slowly in opposite

directions. In this case, the free space between the inner and the outer cylindrical walls is very small which makes the heat transfer occurs by pseudo conduction. An increase in the value of aspect ratio will generate an increase in the air gap. This additional free space will enhance the convection as illustrated in the Figure 6(b) where transfer by natural convection becomes more intensive especially in the upper part of the annular space under the buoyancy effect. Also noted an increasing in the dimensionless velocity values consequently with mentioned that the maximum velocity occurs near the boundary layer of inner cylinder in both left and right sides. In the other hand, with a further increase of the free space that corresponds to A=3, isotherms in Figure 6(c) show that heat transfer remains dominated by a convective mode and the hot air is diffused in more regions of the annular space but with a slight decrease in the intensity of the convection due to the increase in the gap.
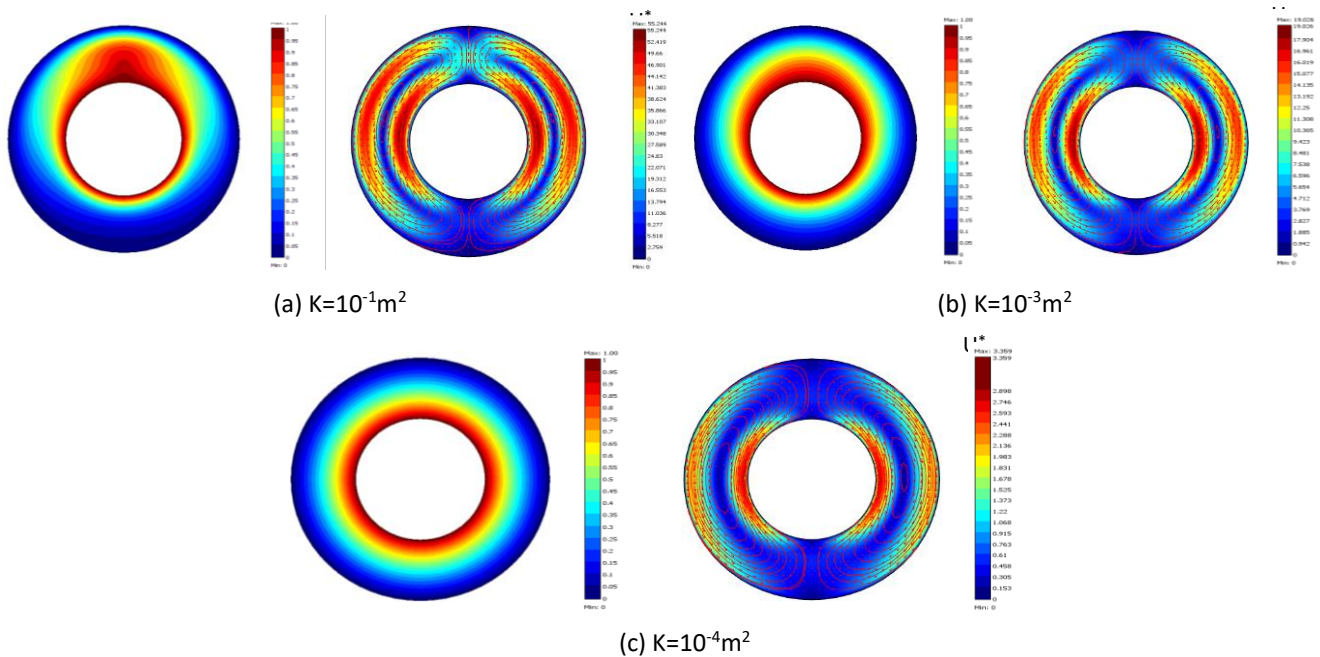

(a) A=1.2   (b) A=2

(c) A=3
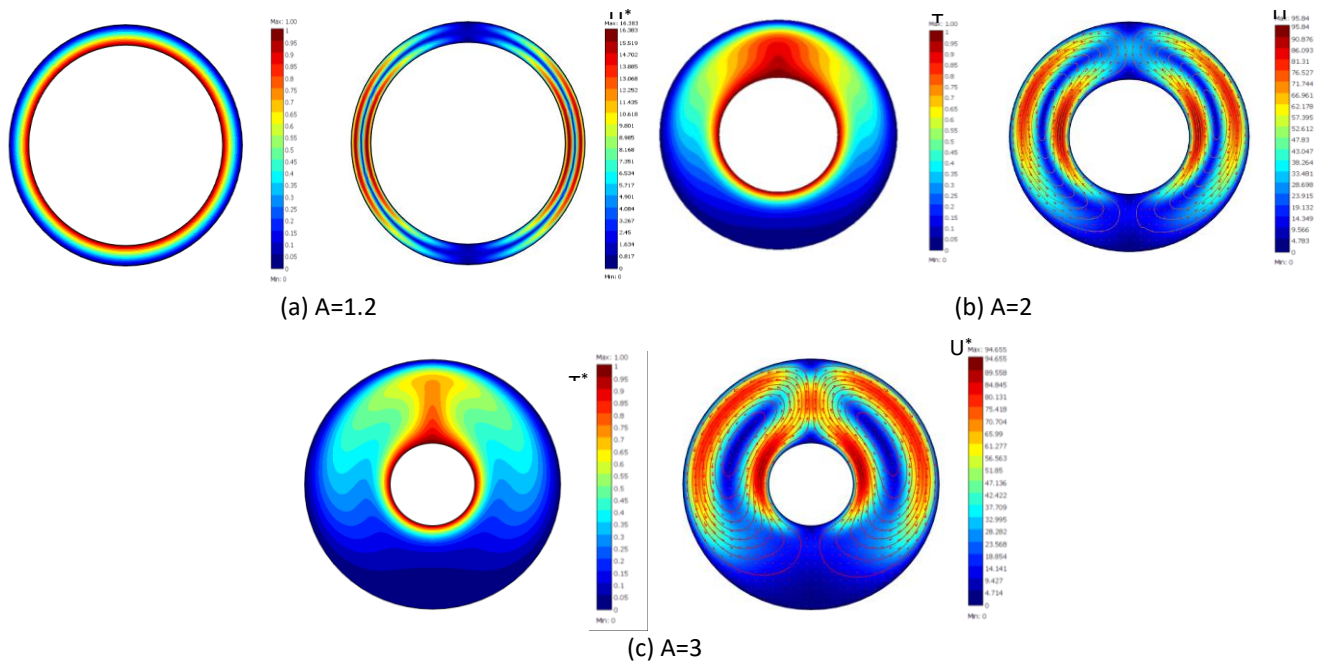
Fig. 6. Isotherms and streamlines for different values of aspect ratio A with Rayleigh number Ra=10^5

3.3. Space Filled with a Fluid-Saturated Porous Medium
3.3.1 Effect of permeability

Figure 7 represents isotherms and streamlines for different permeability values from K=10^{-1}m^2 to K=10^{-4}m^2 for a determined aspect ratio A=2 and Rayleigh number Ra=10^5. We can observe that these contours are symmetrical about the median fictitious vertical plane and the flow is organized in two main cells that rotate in opposite directions. In Figure 7(a) for K=10^{-1}m^2 which is considered high permeability, The isotherms are rising upward which means that heat transfer is dominated by a convective mode in the upper region in contrary to the lower region that still under a pseudo conduction. The velocity field in the same figure shows that the fluid motion is relatively important. The fluid is pushed towards the inner and the outer walls through the porous medium and the convective cells are adjacent in the upper and the lower regions of the annular space. With a decrease in porous medium permeability to K=10^{-3}m^2, Figure 7(b) illustrate that isotherms are recessed to an eccentric closed curves configuration under the diminution of the porous channels which affected the flow by an evident decreasing in the dimensionless velocity values and the pseudo-conductive heat transfer regime becomes preponderant with a slight contribution of the

convection regime. Figure 7(c) shows that with a furthermore decrease in the permeability to K=10^{-4}m^2,The low permeability affects the flow behavior and begin gradually resisting the flow motion until the isotherms become clearly a concentric circles and the pseudo-conduction completely dominates the heat transfer regime in the whole annular space. The velocity field in the same figure exhibits a net decrease in the dimensionless velocity values with the permeability decrease; we can note that flow rotating cells are splaying away in opposite directions leaving a gap in both upper and lower regions due to dominance of the pseudo-conduction in the whole space, this regime is known as creeping flow where the fluid motion is slowed down by the porous medium that is characterized by low permeability.

(a) K=10^{-1}m^2 (b) K=10^{-3}m^2

(c) K=10^{-4}m^2

Fig. 7. Isotherms and streamlines for different values of permeability K with Rayleigh number Ra=10^5 and aspect ratio A=2

4. Conclusions

In the present study, a numerical simulation using COMSOL Multiphysics software was carried out to analyze the convective heat transfer in the horizontal annular space filled with a fluid saturated porous medium. We examined the effect of Rayleigh number that considerably influenced the nature and the structure of the flow; the results have shown that for low Rayleigh number heat transfer is dominated by the pseudo-conduction regime in the whole annular space. But with the increase in its value, the flow becomes more pronounced so the convective regime appears and dominates the heat transfer within the space with an important intensity in the upper part of the annular space particularly. Furthermore, we summarized that heat transfer is improved when the free space between the two cylinders increases what made natural convection have enough space to develop and present further intensification with each additional expansion in the annular space. The permeability effect is also investigated in the second case. On one hand, we have observed that the fluid flow is more significant for high permeability which led to high velocity gradients and allows the convection to intensify in the upper part of the horizontal annular space. On the other hand, low permeability inhabited the flow inside the annular enclosure and led to a

relatively slow fluid motion. In this case heat transfer is completely dominated by the pseudo conductive regime due to the high flow resistance.

References

[1] Wakid, Muhkamad, Aan Yudianto, and Agus Widyianto. "Numerical Modelling and Analysis of Externally Blown Heated Pipes Applicable for Furnace." *Journal of Advanced Research in Fluid Mechanics and Thermal Sciences* 100, no. 1 (2022): 30-43. https://doi.org/10.37934/arfmts.100.1.3043

[2] Jung, Eui Guk, and Joon Hong Boo. "A Novel Analytical Modeling of a Loop Heat Pipe Employing the Thin-Film Theory: Part I—Modeling and Simulation." *Energies* 12, no. 12 (2019): 2408. https://doi.org/10.3390/en12122408

[3] Albeshri, Badr Ali Bzya, Nazrul Islam, Ahmad Yahya Bokhary, and Amjad Ali Pasha. "Hydrodynamic Analysis of Laminar Mixed Convective Flow of Ag-TiO2-Water Hybrid Nanofluid in a Horizontal Annulus." *CFD Letters* 13, no. 7 (2021): 47-57. https://doi.org/10.37934/cfdl.13.7.4557

[4] Sun, K. H., and C. L. Tien. "Thermal performance characteristics of heat pipes." *International Journal of Heat and Mass Transfer* 18, no. 3 (1975): 363-380. https://doi.org/10.1016/0017-9310(75)90026-5

[5] Ja, A., J. Belabid, and A. Cheddadi. "Heat and mass transfer in a saturated porous medium confined in cylindrical annular geometry." *International Journal of Mechanical, Aerospace, Industrial and Mechatronics Engineering* 9, no. 4 (2015): 525-529. https://doi.org/10.5281/zenodo.1100336

[6] Elfaghi, Abdulhafid MA, Alhadi A. Abosbaia, Munir FA Alkbir, and Abdoulhdi AB Omran. "CFD Simulation of Forced Convection Heat Transfer Enhancement in Pipe Using Al2O3/Water Nanofluid." *Journal of Advanced Research in Numerical Heat Transfer* 8, no. 1 (2022): 44-49. https://doi.org/10.37934/cfdl.14.9.118124

[7] Kumar, Vikas, D. Gangacharyulu, and Ram Gopal Tathgir. "Heat transfer studies of a heat pipe." *Heat Transfer Engineering* 28, no. 11 (2007): 954-965. https://doi.org/10.1080/01457630701421810

[8] Blet, Nicolas, Stéphane Lips, and Valérie Sartre. "Heats pipes for temperature homogenization: A literature review." *Applied Thermal Engineering* 118 (2017): 490-509. https://doi.org/10.1016/j.applthermaleng.2017.03.009

[9] Braga, Edimilson J., and Marcelo JS De Lemos. "Simulation of turbulent natural convection in a porous cylindrical annulus using a macroscopic two-equation model." *International journal of heat and mass transfer* 49, no. 23-24 (2006): 4340-4351. https://doi.org/10.1016/j.ijheatmasstransfer.2006.04.032

[10] Boulechfar, Hichem, Mahfoud Djezzar, and Amel Labed. "Effect of eccentricity on natural convection in fluid-saturated porous media in an elliptical annulus." *Mechanics & Industry* 16, no. 4 (2015): 403. https://doi.org/10.1051/meca/2015015

[11] Famouri, Mehdi. "Numerical analysis of phase change, heat transfer and fluid flow within miniature heat pipes." PhD diss., University of South Carolina, 2017.

[12] Hussain, Mohammed Noorul, and Isam Janajreh. "Numerical simulation of a cylindrical heat pipe and performance study." *Int. J. of Thermal & Environmental Engineering* 12, no. 2 (2016): 135-141. https://doi.org/10.5383/ijtee.12.02.010

[13] Ma'a, Mustaza, Indro Pranoto, and Samsul Kamal. "The Phenomenon of Flow and Heat Transfer in Annular Heat Exchanger on Plain Tube Condition." *Journal of Advanced Research in Fluid Mechanics and Thermal Sciences* 100, no. 2 (2022): 146-156. https://doi.org/10.37934/arfmts.100.2.146156

[14] Al-Hattab, Tahseen A., Majid H. Majeed, and Mushtaq F. Abd-Saada. "Heat Transfer By Free Convection Between Horizontal Concentric Pipes." *The Iraqi Journal For Mechanical And Material Engineering* 8, no. 3 (2008): 219-236.

[15] Yang, Xiufeng, and Song-Charng Kong. "Numerical study of natural convection states in a horizontal concentric cylindrical annulus using SPH method." *arXiv preprint arXiv:1712.05831* (2017). https://doi.org/10.1016/j.enganabound.2019.02.007

[16] Yuan, Xing, Fatemeh Tavakkoli, and Kambiz Vafai. "Analysis of natural convection in horizontal concentric annuli of varying inner shape." *Numerical Heat Transfer, Part A: Applications* 68, no. 11 (2015): 1155-1174. https://doi.org/10.1080/10407782.2015.1032016